Available online at www.sciencedirect.com
SCIENCE DIRECT®
Chemical Physics Letters 387 (2004) 301–306
CHEMICAL PHYSICS LETTERS
www.elsevier.com/locate/cplett

Resonant Raman spectra of carbon nanotube bundles observed by perpendicularly polarized light

A. Grüneis [a,*], R. Saito [a], J. Jiang [a], Ge.G. Samsonidze [b], M.A. Pimenta [e], A. Jorio [c,e], A.G. Souza Filho [c,f], G. Dresselhaus [d], M.S. Dresselhaus [b,c]

[a] Department of Physics, Tohoku University and CREST, JST, Aoba, Sendai 980-8578, Japan
[b] Department of Electrical Engineering and Computer Science, Massachusetts Institute of Technology, Cambridge, MA 02139-4307, USA
[c] Department of Physics, Massachusetts Institute of Technology, Cambridge, MA 02139-4307, USA
[d] Francis Bitter Magnet Laboratory, Massachusetts Institute of Technology, Cambridge, MA 02139-4307, USA
[e] Departamento de Física, Universidade Federal de Minas Gerais, Belo Horizonte – MG 30123-970, Brazil
[f] Departamento de Física, Universidade Federal do Ceará, Fortaleza – CE 60455-760, Brazil

Received 15 December 2003; in final form 13 February 2004
Published online: 5 March 2004

Abstract

We calculated the resonance condition for the radial breathing Raman mode for single wall carbon nanotube (SWNT) bundles for light polarization parallel and perpendicular to the tube axis. The radial breathing modes that are not observed in isolated SWNTs, but are observed in SWNT bundles, are assigned to a resonance process for light with perpendicular polarization. Asymmetry between the valence and conduction π energy bands becomes essential for obtaining resonance conditions. We find that due to a high joint density of states, armchair SWNTs have the largest optical transition intensities.

1. Introduction

Raman spectra at the single nanotube level has provided a standard tool for assigning (n, m) values of single wall carbon nanotubes (SWNTs) as a quick, non-contact, non-destructive room-temperature measurement with high energy resolution on the order of 10 meV [1,2]. When we observe the Raman spectra from an isolated SWNT by changing the polarization of the light, usually there is no signal for light with a polarization perpendicular to the nanotube axis [3–6]. Thus in the assignment of (n, m) values, we have only considered the resonant condition for the light polarized parallel to the nanotube axis [2]. In fact, this assignment is sufficient for explaining most of the Raman spectra we have observed for *isolated* SWNTs on a SiO_2 substrate by using the previously fitted nearest neighbor tight-binding parameter $\gamma_0 = 2.89$ eV and the dependence of the radial breathing mode (RBM) frequency ω_{RBM} (in cm^{-1}) on the diameter d_t ($1 < d_t < 2$ nm), for which the relation, $\omega_{RBM} = 248/d_t$ is usually employed [2]. However, when we try to use the same method for the RBM spectra for nanotube *bundles*, we found that some RBM spectra cannot be assigned simply by changing the values of the above parameters for the bundles or by adding a term to account for tube–tube interactions [7]. Such a term shifts the RBM frequency up by only about 10 cm^{-1} as compared to an isolated SWNT, depending on the SWNT diameter and the number of SWNTs in the bundle [8,9]. Although the tube–tube interaction between SWNTs in a bundle may change the electronic and phonon structures, the modifications of the electronic or phonon energy band structures from those of an isolated SWNT are not so drastic for tubes with $d_t > 0.9$ nm as to explain the unassigned Raman spectra. In fact, the diameter change corresponding to a 14 cm^{-1} RBM shift is $\Delta d_t = 0.05$ nm, and thus this change does not produce an (energy, d_t) point in the energy gap

* Corresponding author. Fax: +81-222-176475.
E-mail address: alex@flex.phys.tohoku.ac.jp (A. Grüneis).

0009-2614/$ - see front matter © 2004 Elsevier B.V. All rights reserved.
doi:10.1016/j.cplett.2004.02.034

region in the Kataura plot for resonance Raman energy [2,10,11]. Since the unexplained features appear at energies that are very different from the resonances observed for isolated SWNTs, a simple adjustment of tight-binding parameters cannot account for this data [12]. Thus, within the Raman process occurring for parallel polarized light, we cannot explain all the RBM data observed only in SWNT bundles, though the data for isolated SWNTs can be explained.

In order to explain the unassigned peaks, we examine here the possibility for a resonance Raman process with perpendicularly polarized light. To compare our predictions with experimental data, we take data of previously published RBM Raman spectra [13], and obtain the resonant diameters for a given laser energy using the ω_{RBM} dependence on d_{t}. The absence of optical absorption for perpendicularly polarized light has been previously explained by the depolarization effect [14] according to which the self-consistently induced charge appearing on the surface of a SWNT in the presence of an electric field perpendicular to the nanotube axis cancels the field of the incident light. This screening effect depends on the geometry of the nanotubes, and it is thus expected that in a SWNT bundle the screening effect is not perfect, since the depolarization field from the neighboring nanotubes may smear out the perfect cancellation of the electric field that occurs for isolated SWNTs in vacuum. Thus, even for an isolated SWNT on an SiO_2 surface, this perfect cancellation might not occur because of the surface effect of the dielectric Si substrate. However, the dipole selection rule tells us that the resonance energy for perpendicularly polarized light is different from that for parallel polarization [3]. In order to check whether we get resonant Raman spectra from an isolated nanotube for perpendicularly polarized light or not, we need not only rotate the polarization direction, but we must also change the laser excitation energy, since the resonance energy for perpendicularly polarized light is different from that for parallel polarized light.

In this Letter, we consider the resonance condition as a function of diameter (the so-called Kataura plot [10,11]) for perpendicularly polarized light, and we find that this new resonant condition works well for explaining features of the RBM spectra observed only in SWNT bundles and not observed for isolated SWNTs. Although we have not yet calculated the depolarization effect of the bundle, the possible use of perpendicular polarized light in experiments on SWNT bundle samples is important for the study of Raman spectroscopy in SWNTs.

2. Selection rules for optical absorption in SWNTs

The electronic π bands in SWNTs are commonly calculated by zone-folding of the electronic π bands of two dimensional (2D) graphite $E^{j}_{\mathrm{g\,2D}}(k)$ [15],

$$E^{j}_{\mu}(k) = E^{j}_{\mathrm{g\,2D}}\left(k\frac{\mathbf{K}_2}{|\mathbf{K}_2|} + \mu\mathbf{K}_1\right), \quad j = v \text{ or } c,$$
$$\mu = 0,\ldots,N-1, \text{ and } -\frac{\pi}{T} < k < \frac{\pi}{T}. \tag{1}$$

This involves one-dimensional (1D) k states along so-called cutting lines [16] in k space. Cutting lines are the 1D Brillouin zone (BZ) and labeled by an index μ in Eq. (1), so that $\mu\mathbf{K}_1$ is the normal vector from the Γ point of graphite to the cutting lines. Each μ gives two bands, a valence and a conduction band, denoted by $E^{\mathrm{v}}_{\mu}(k)$ and $E^{\mathrm{c}}_{\mu}(k)$, respectively. The dipole selection rules have been derived for linearly polarized light propagating perpendicular to the tube axis [14,17] and for circularly polarized light propagating along the tube axis [18,19]. Depending on the light polarization, it is shown that we get different final electron states for dipole allowed transitions. Thus, also the resonant energies are generally different for different scattering geometries so that the orientation of the SWNT on the substrate must be considered, when analyzing optical absorption or Raman spectra. The transition probability is given by a sum over initial electron states μ_{i}, k_{i} and a final electron states μ_{f}, k_{f} that are in resonance with E_{laser} and can be expressed as

$$W(E_{\mathrm{laser}}) = \frac{e^2\hbar^3 I}{\epsilon c m^2 E^2_{\mathrm{laser}}} \times \sum_{\mu_{\mathrm{i}}}\int_{-\pi/T}^{\pi/T} \mathrm{d}k_{\mathrm{i}} \left| \sum_{\mu_{\mathrm{f}}}\int_{-\pi/T}^{\pi/T} \mathrm{d}k_{\mathrm{f}} \mathbf{D}(\mu_{\mathrm{f}},k_{\mathrm{f}},\mu_{\mathrm{i}},k_{\mathrm{i}})\cdot\mathbf{P} \times \delta(E^{\mathrm{c}}_{\mu_{\mathrm{f}}}(k_{\mathrm{f}}) - E^{\mathrm{v}}_{\mu_{\mathrm{i}}}(k_{\mathrm{i}}) - E_{\mathrm{laser}})\delta(k_{\mathrm{f}} - k_{\mathrm{i}}) \right|^2, \tag{2}$$

in which e, m, I, ϵ and $\mathbf{P}$ are the electron charge, electron mass, the intensity of the incident light, the dielectric constant and the light polarization, respectively. $\mathbf{D}$ is the SWNT dipole vector defined by [17]:

$$\mathbf{D}(\mu_{\mathrm{f}},k_{\mathrm{f}},\mu_{\mathrm{i}},k_{\mathrm{i}}) = \langle \Psi^{\mathrm{c}}(\mathbf{r},\mu_{\mathrm{f}},k_{\mathrm{f}}) | \nabla | \Psi^{\mathrm{v}}(\mathbf{r},\mu_{\mathrm{i}},k_{\mathrm{i}}) \rangle, \tag{3}$$

where Ψ^{c} and Ψ^{v} are wavefunctions for conduction and valence band, respectively. Hereafter we take the z axis in the direction of the SWNT axis. If $\mu_{\mathrm{f}} = \mu_{\mathrm{i}} \pm 1$, $\mathbf{D}$ has non-zero x and y components, but $D_z = 0$. If $\mu_{\mathrm{f}} = \mu_{\mathrm{i}}$, then only the z component of $\mathbf{D}$ becomes non-zero. In both cases the 1D wavenumber is conserved, i.e. $k_{\mathrm{f}} = k_{\mathrm{i}}$ because of the second δ function in Eq. (2). Thus, to get $\mu_{\mathrm{f}} = \mu_{\mathrm{i}} \pm 1$ or $\mu_{\mathrm{f}} = \mu_{\mathrm{i}}$, we need $\mathbf{P}$, that has x and y or a z component which corresponds to perpendicular or parallel polarizations, respectively. $\mathbf{D}$ becomes a zero vector for other cases of μ_{i} and μ_{f}. In Eq. (2) the allowed dipole transitions which have the same energy from one given initial k_{i} state can interfere with one another [20]. The interference for linearly polarized light can only occur for light polarization perpendicular to the tube axis, because only for this light polarization can the electron go to two

different final states ($\mu \rightarrow \mu \pm 1$). However the interference only occurs if the transition energies are equal because of the δ function in Eq. (2). Thus we must square the matrix element after adding all contributions that originate from the same initial wavevector. In Fig. 1a the initial and final states for transitions with perpendicularly polarized light are shown for a (10,2) semiconducting SWNT of type II [16]. Only transitions related to van Hove singularities (vHS) in the joint density of states (JDOS) are shown. For parallel polarization, the vHS are denoted by $\mathbf{k}_i$ (with $i = 1, 2, 3$), in which the van Hove singularity k point is expressed by a touching of the cutting lines to the equi-energy contour. The energy gaps between valence and conduction bands at each $\mathbf{k}_i$ point are usually labelled E_{ii}^{M} and E_{ii}^{S}, where the i orders the transition energy magnitude in increasing order, and M and S denote metallic and semiconducting SWNTs, respectively. These energies are usually observed with parallel polarized light and plotted vs. d_{t} in a Kataura plot [10]. In the case of perpendicular polarization, the k, that contributes to the JDOS, is the point where the valence and conduction bands have the same slope. Generally, these points occur for a 1Dk value in between the 1D k_i vHS wavenumbers for adjacent cutting lines. Hereafter we use k_{ij} to denote the 1D wavenumber at which the vHS transitions between cutting lines of the E_{ii} and E_{jj} singularities occur. There are in general two vHS-enhanced transitions starting from a given initial μ index as is shown by labels (p1) and (p2) in Fig. 1a. In Fig. 1a, only transitions originating from the μth line are considered and illustrated by arrows, pointing towards the $\mu \pm 1$ cutting lines:

$$\begin{aligned} &(\mathrm{p1}) \quad E_{12}^{\mathrm{S}} = E_{\mu-\ell}^{\mathrm{c}}(k_{12}) - E_{\mu}^{\mathrm{v}}(k_{12}), \\ &(\mathrm{p2}) \quad E_{13}^{\mathrm{S}} = E_{\mu+\ell}^{\mathrm{c}}(k_{13}) - E_{\mu}^{\mathrm{v}}(k_{13}). \end{aligned} \tag{4}$$

In Eq. (4) we use the label E_{ij}^{S} for a semiconducting SWNT, for which the electron goes from E_{μ}^{v} to $E_{\mu+\ell}^{\mathrm{c}}$. Here, the cutting line with index μ has the E_{ii} singularity and the cutting line with index $\mu + \ell$ has the E_{jj} singularity. The parameter $\ell = \pm 1$, depends on which of the two inequivalent corners of the 2D BZ, K or K', the transition occurs, and whether the SWNT is semiconducting type I or II. In Eq. (4) we have selected the two transitions that start from the cutting line with the E_{11} singularity. In Eq. (4) we have $\ell = 1$ for a semiconducting type I tube for k_{ij} on μ cutting line near the K point. When we select μ around K' we get $\ell = -1$. For a semiconducting type II SWNT, the situation is just the opposite and we get $\ell = -1$ ($\ell = 1$) for μ near the K (K') point. The two transitions in Eq. (4) are shown in Fig. 1a. When we consider relatively small transition energies, we can neglect both the trigonal warping effect and the electron–hole asymmetry. Then we can use the following simplification:

$$E_{12}^{\mathrm{S}} = \frac{E_{22}^{\mathrm{S}} + E_{11}^{\mathrm{S}}}{2}, \quad E_{13}^{\mathrm{S}} = \frac{E_{33}^{\mathrm{S}} + E_{11}^{\mathrm{S}}}{2}. \tag{5}$$

Thus the resonance energy E_{12}^{S} for perpendicular polarization appears in the energy gap of E_{11}^{S} and E_{22}^{S}, as is shown in Fig. 1b. Similar results can be obtained for other transitions. The splitting of the E_{11}^{S} transition is however somewhat special, since both E_{12}^{S} and E_{13}^{S} are larger than E_{11}^{S}. So far we assumed that the overlap parameter s vanishes ($s = 0$) in calculating the electron energy dispersion in the tight-binding calculation [15]. A non-zero s value is essential for obtaining a larger (smaller) energy band width in the conduction (valence) bands. However, as far as we consider parallel polarization, an enlargement of the conduction band width and a shrinking of the valence band width for the same μ value cancel each other to linear order in s, and the effect of s will only appear to order s^2. Thus for the value of $s = 0.129$, this effect can be neglected around the K point of the 2D BZ [11]. However, it is no longer true for perpendicular polarization. The energy difference

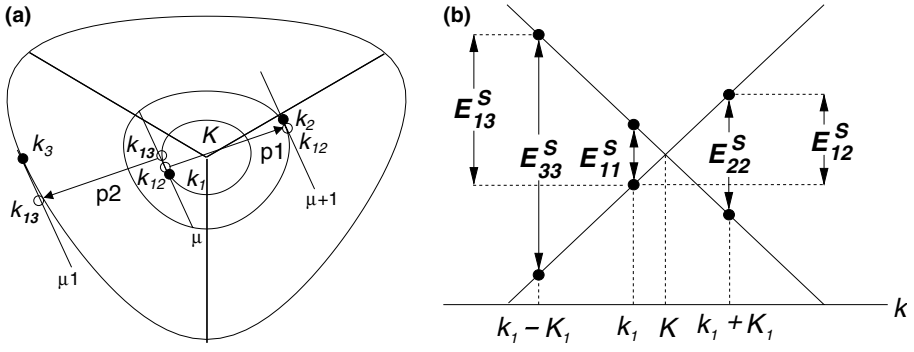

Fig. 1. (a) The three parallel lines labelled by $\mu - 1$, μ and $\mu + 1$ are cutting lines for a (10,2) tube near the K point. For parallel light polarization, transitions occur at vHS k points k_1, k_2 and k_3, denoted by a filled circle, and for perpendicular polarization, the k_{12} and k_{13}, are indicated by open circles. For perpendicular polarization, the two transitions at vHS in the JDOS, labeled by p1 and p2 are shown [Eq. (4)]. (b) Energy dispersion along 2D $\mathbf{k}$ parallel to $\mathbf{K}_1$. The energies at the vHSs $\mathbf{k}_i$ are denoted by E_{ii}. If we neglect the trigonal warping effect and electron–hole asymmetry, the resonant energies for perpendicular polarization are given by E_{12}^{S} and E_{13}^{S}.

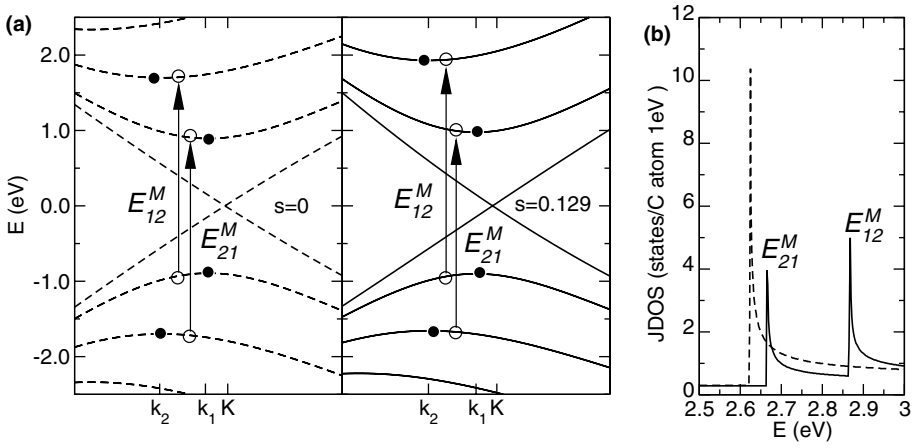

Fig. 2. The electron–hole asymmetry leads to different energies for the electronic transitions for perpendicularly polarized light. In (a) we show $E(k)$ for a (10,10) tube around the K point. The dashed lines (left) are for tight binding parameters $t = -2.89$ eV and $s = 0$ and for the solid lines (right) $t = -3.033$ eV and $s = 0.129$ was used. (b) JDOS for transitions with perpendicularly polarized light for a (10,10) SWNT. The dashed and solid lines in (b) are the calculated absorption spectra for (a) left and right, respectively.

between E_{ij} and E_{ji} depends on the amount of the electron–hole asymmetry, which is contained in the tight-binding overlap parameter s. In Fig. 2a we show an example of the band structures of a (10,10) metallic SWNT with $s = 0$ (left) and $s = 0.129$ (right). Solid circles indicate vHS **k** points. In Fig. 2b we plot the JDOS for these band structures. We find a splitting between the E_{12} and E_{21} transition energies when $s \neq 0$ (solid line). For $s = 0$, the E_{12} and E_{21} transitions occur at the same energies (dashed line). The splitting in $E_{12} - E_{21}$ for $s = 0.129$ is about 0.2 eV and thus should be observable in optical experiments. Alternatively, the dependence $E_{12} - E_{21}$ on s could be used to determine the exact value of s for different SWNT diameters.

3. Katauras plot for perpendicular polarization

We now discuss the SWNT diameter dependence of the transition energies in the Kataura plot. This plot is usually done for parallel polarization and the E_{ii} are plotted vs. SWNT diameters d_t. Experimentally the E_{ii} energies can be obtained by Raman experiments, using a tunable laser [1] or by comparing Stokes and anti-Stokes intensities [21] or by photoluminescence (PL) experiments [22], where the ratio between two E_{22} and E_{11} can be determined. Alternatively, we can also take peaks in the RBM Raman spectra of bundles and assign them to resonance of a particular SWNT diameter with E_{laser}. In this way we analyzed the experimental data we use. The experimental points have been measured using six different E_{laser}: 1.17, 1.59, 1.92, 2.41, 2.54 and 2.71 eV [13]. In order to compare them to the calculated Kataura plot for parallel and perpendicular polarization, shown in Fig. 3a and in b, respectively, we plot the same set of experimental points 'X' in Fig. 3a and in b. Each 'X' corresponds to a peak in the RBM Raman spectra of randomly aligned bundles. If we assume only resonance for parallel polarization, we would expect each 'X' to lie in a region of E_{ii} points. However, when we plot all features, that appear in the experimental spectra of SWNT bundles, several small intensity peaks that cannot be explained by this method, since they appear in the gap region of E_{ii} transitions in Fig. 3a. Comparison with calculated values of vHS energies of perpendicular polarization suggests that an 'X', that lies in between two E_{ii} regions in Fig. 3a, lies in an E_{ij} region in Fig. 3b. This most clearly holds for the experimental data around 1.6 eV, which are in the gap region between E_{22}^{S} and E_{11}^{M}. Most of these points can be seen to be far (i.e. $\sim$0.2 eV) from the E_{22}^{S} and E_{11}^{M} transitions but do lie in the E_{13}^{S} region. We thus assign these experimental data points to the E_{13}^{S} transition with perpendicular polarization. Such an assignment holds, even when we consider the resonance window of E_{ii} with E_{laser}, that has been neglected, when we simply assign the E_{ii} equal to E_{laser}. Also an upshift of E_{22}^{S} by roughly 0.2 eV [22], that has been reported recently, would only change the assignment to E_{13}^{S} for a few but not all points. Smaller E_{laser} data around 1.2 eV may consist of E_{22}^{S} (parallel polarization) or E_{12}^{S} and E_{10}^{M} (perpendicular polarization). When we go to energies above 2.2 eV, the situation is no longer so clear, and the orientation of the resonant SWNTs with respect to the light polarization should be known in order to make an assignment for transitions with parallel or perpendicular polarization.

4. Dipole matrix element

It is important to discuss the intensity of the dipole transitions since PL show some (n, m) SWNTs that give

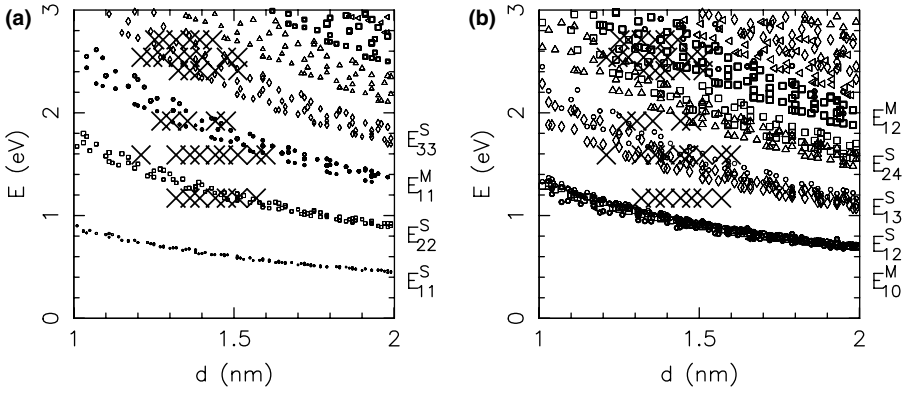

Fig. 3. Energies of van Hove singularities vs. tube diameter for (a) parallel polarization and (b) perpendicular polarization. In (a) the transitions are indicated as follows: (○) E^S_{11}, (□) E^S_{22}, (●) E^M_{11}, (◇) E^S_{33}, (△) E^S_{44}, (■) E^M_{22}, (◁) E^S_{55}. In (b) we use the same symbols to denote the initial state and plot transitions that have a vHS in the JDOS for neighbouring cutting lines. The 'X' show experimental data for SWNT bundles [13]. The plots are made for the values of $t = -3.033$ eV and $s = 0.129$.

a relatively large intensity. The PL intensity spectra can be understood in terms of a product of two matrix elements at opposite sides of the K point for absorption and emission of light. Here we however only consider optical absorption and emission at one given k, which is related to the PL experiments. There are three reasons for the (n,m) dependence of the optical absorption. Firstly, we have a term E^2_{laser} in the denominator of Eq. (2). Secondly, the JDOS at a given energy can be large, since several vHS transitions appear at the same energy. Further, the distance of the vHS k point from K affects the JDOS, since energy bands become flatter for larger distances from K. Thirdly, the matrix element in Eq. (3) has a $\mathbf{k}$ (and thus an energy) dependence. When we evaluate Eq. (2), all effects are included. In Fig. 4, we plot the value of the transition probability $W(E_{\text{laser}})$ as a function of E_{laser} for vHS-resonant SWNTs. Transitions with parallel and perpendicularly polarized light are shown in Fig. 4a and b, respectively. Because the singularities in the JDOS for perpendicular polarization appear at k_{ij}, which are in between k_i and k_j, the number of E_{ij} is larger by about a factor 2 compared to the number of E_{ii} points.

The strongest influence on W is due to the E^2_{laser} term in the denominator of Eq. (2) and we generally expect a decrease of W with increasing E_{laser}. Nevertheless, we can observe effects due to the JDOS or the matrix element. Since the effect of the JDOS is particularly large for armchair SWNTs, the transitions with high intensity come preferentially from armchair chiralities ($\theta \sim 30°$). Armchair SWNTs have four vHS at the same energy, whereas other SWNTs generally only have two vHS at

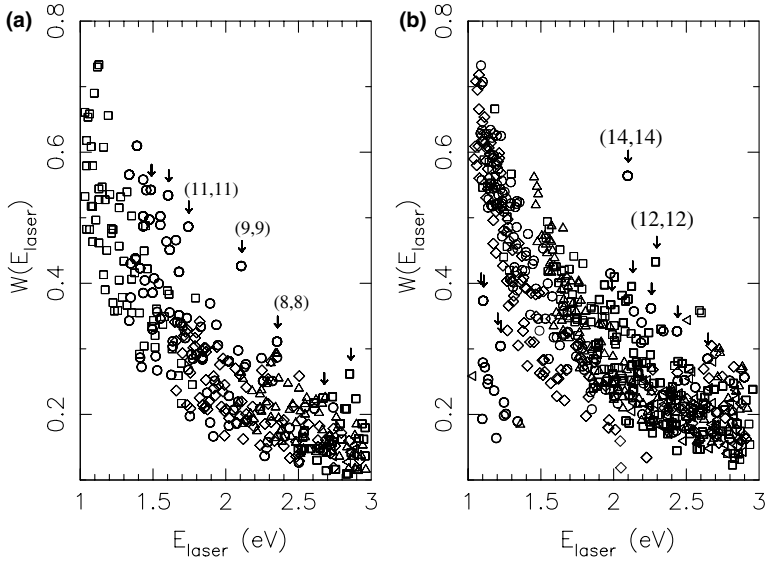

Fig. 4. Energy dependence of the optical absorption intensity W is shown in (a) for parallel polarization and in (b) for perpendicular polarization as a function of E_{laser} for SWNTs with diameters d_t $1 < d_t < 2$ nm. Symbols have the meaning as in Fig. 3. Arrows indicate armchair SWNTs of which a few a denoted by (n,m) indices.

the same energy since there is no trigonal warping effect in armchair SWNTs [11].

5. Conclusion

In conclusion, we analyzed SWNT RBM Raman spectra and assigned the features, that could not be explained by transitions with parallel polarized light to a resonance that is only possible for the light polarization perpendicular to the SWNT axis. Such resonances could be assigned, if the energies were clearly between the resonant energies for parallel polarization, so that a small shift of tight binding parameters does not affect the result. Furthermore, when a SWNT is in resonance with perpendicularly polarized light, the transition energies between different subbands show a small, but observable splitting which depends on the electron hole asymmetry. This result provides new research directions for both theory and experiment. The resonance condition for light with perpendicular polarization can be used for the interpretation of polarized optical absorption, photoluminescence and Raman spectra. We showed that the energy difference between E_{ij} and E_{ji} transitions results from the asymmetry between the valence and conduction bands. This energy difference can be measured in future experiments.

Acknowledgements

A.G. acknowledges financial support from the Ministry of Education, Japan. R.S. and G.S.M. acknowledge a Grant-in-Aid (No. 13440091) from the Ministry of Education, Japan. A.J./A.G.S.F. acknowledge support from the Brazilian agencies CNPq/CAPES. The MIT authors acknowledge support under NSF Grants DMR 01-16042 and INT 00-00408.

References

[1] M.S. Dresselhaus, G. Dresselhaus, A. Jorio, A.G. Souza Filho, R. Saito, Carbon 40 (2002) 2043.
[2] A. Jorio, R. Saito, J.H. Hafner, C.M. Lieber, M. Hunter, T. McClure, G. Dresselhaus, M.S. Dresselhaus, Phys. Rev. Lett. 86 (2001) 1118.
[3] G.S. Duesberg, I. Loa, M. Burghard, K. Syassen, S. Roth, Phys. Rev. Lett. 85 (2000) 5436.
[4] J. Hwang, H.H. Gommans, A. Ugawa, H. Tashiro, R. Haggenmueller, K.I. Winey, J.E. Fischer, D.B. Tanner, A.G. Rinzler, Phys. Rev. B 62 (R13) (2000) 310.
[5] Z. Yu, L.E. Brus, J. Phys. Chem. B 105 (2001) 1123.
[6] A. Jorio, A.G. Souza Filho, G. Dresselhaus, M.S. Dresselhaus, A.K. Swan, M.S. Ünlü, B.B. Goldberg, M.A. Pimenta, J.H. Hafner, C.M. Lieber, R. Saito, in: P. Nikolaev, P. Bernier, P. Ajayan, Y. Iwasa (Eds.), Making Functional Materials with Carbon Nanotubes: MRS Symposium Proceedings, Boston, December 2001, Materials Research Society Press, Pittsburgh, PA, 2002, p. Z6.19.
[7] U.D. Venkateswaran, A.M. Rao, E. Richter, M. Menon, A. Rinzler, R.E. Smalley, P.C. Eklund, Phys. Rev. B 59 (1999) 10928.
[8] L. Henrard, E. Hernández, P. Bernier, A. Rubio, Phys. Rev. B 60 (1999) R8521.
[9] H. Kuzmany, W. Plank, M. Hulman, C.h. Kramberger, A. Grüneis, T.h. Pichler, H. Peterlik, H. Kataura, Y. Achiba, Eur. Phys. J. B 22 (2001) 307.
[10] H. Kataura, Y. Kumazawa, Y. Maniwa, I. Uemezu, S. Suzuki, Y. Ohtsuka, Y. Achiba, Synt. Met. 103 (1999) 2555.
[11] R. Saito, G. Dresselhaus, M.S. Dresselhaus, Phys. Rev. B 61 (2000) 2981.
[12] S. Maruyama, Y. Miyauchi, Y. Murakami, S. Chiashi, New J. Phys. 5 (2003) 149.1.
[13] M.A. Pimenta, A. Marucci, S.D.M. Brown, M.J. Matthews, A.M. Rao, P.C. Eklund, R.E. Smalley, G. Dresselhaus, M.S. Dresselhaus, J. Mater. Res. 13 (1998) 2396.
[14] H. Ajiki, T. Ando, Phys. B Condens. Matter 201 (1994) 349.
[15] R. Saito, G. Dresselhaus, M.S. Dresselhaus, Physical Properties of Carbon Nanotubes, Imperial College Press, London, 1998.
[16] Ge.G. Samsonidze, R. Saito, A. Jorio, M.A. Pimenta, A.G. Souza Filho, A. Grüneis, G. Dresselhaus, M.S. Dresselhaus, J. Nanosci. Nanotechnol. (2003).
[17] A. Grüneis, R. Saito, Ge.G. Samsonidze, T. Kimura, M.A. Pimenta, A. Jorio, A.G. Souza Filho, G. Dresselhaus, M.S. Dresselhaus, Phys. Rev. B 67 (2003), 165402-1–165402-7.
[18] E.L. Ivchenko, B. Spivak, Phys. Rev. B 66 (2002) 155404.
[19] Ge.G. Samsonidze, A. Grüneis, R. Saito, A. Jorio, M.A. Pimenta, A.G. Souza Filho, G. Dresselhaus, M.S. Dresselhaus, Phys. Rev. B (2003).
[20] R.M. Martin, L.M. Falicov, Light scattering in solids, in: M. Cardona (Ed.), Topics in Applied Physics, vol. 8, Springer-Verlag, Berlin, 1981.
[21] A.G. Souza Filho, S.G. Chou, G.G. Samsonidze, G. Dresselhaus, M.S. Dresselhaus, A. Lei, J. Liu, Anna K. Swan, M.S. Ünlü, B.B. Goldberg, A. Jorio, A. Grüneis, R. Saito, Phys. Rev. B (2004).
[22] R.B. Weisman, S.M. Bachilo, Nano Lett. (Commun.) 3 (2003) 1235.